


Article

# Numerical Analysis of Energy Recovery of Hybrid Loader Actuators Based on Parameters Optimization

Hongyun Mu , Yanlei Luo \*, Yu Luo and Lunjun Chen

School of Mechanical Engineering, Guizhou University, Guiyang 550025, China

\* Correspondence: ylluo@gzu.edu.cn; Tel.: +86-180-9602-2669

**Abstract:** The conventional loader actuator hydraulic system suffers from the potential energy waste problem of the boom arm. This study proposes a hydraulic control method and control strategy for the energy recovery and regeneration of a hybrid loader arm. When the boom arm drops, the piston side of the boom cylinder charges the accumulator, and the system achieves energy recovery. When the boom arm rises, the accumulator releases hydraulic energy to drive the energy regeneration hydraulic motor to provide energy for the system, and the system achieves energy regeneration. The system's principle analysis and the mathematical model are completed based on Boyle's, Newton's second law, and the flow continuity principle. The simulation model is established using AMESim 2D mechanical library, HCD library, and signal library. Under the typical working condition, 50-type wheel loader numerical simulation research is conducted, and the system cylinder motion characteristics, accumulator charging and discharging performance, system energy recovery, and regeneration performance are obtained. On this basis, energy recovery and regeneration efficiency are selected as optimization objectives. The optimal designs of accumulator and energy regeneration hydraulic motor parameters are carried out to obtain the influence law of accumulator and hydraulic motor parameters on system energy recovery and regeneration, and the energy-saving effect of the system is analyzed. The results show that the optimized parameters effectively improve the system energy recovery and regeneration efficiency and reduce engine fuel consumption. The system provides a reference for designing an energy recovery system and researching the energy-saving technology of loaders.

**Keywords:** hybrid loader; boom arm; accumulator; energy recovery and regeneration; parameters optimization; AMESim simulation



**Citation:** Mu, H.; Luo, Y.; Luo, Y.; Chen, L. Numerical Analysis of Energy Recovery of Hybrid Loader Actuators Based on Parameters Optimization. *Actuators* **2022**, *11*, 260. <https://doi.org/10.3390/act11090260>

Academic Editor: Eihab M. Abdel-Rahman

Received: 31 July 2022  
Accepted: 6 September 2022  
Published: 8 September 2022

**Publisher's Note:** MDPI stays neutral with regard to jurisdictional claims in published maps and institutional affiliations.



**Copyright:** © 2022 by the authors. Licensee MDPI, Basel, Switzerland. This article is an open access article distributed under the terms and conditions of the Creative Commons Attribution (CC BY) license (<https://creativecommons.org/licenses/by/4.0/>).

## 1. Introduction

In recent years, the demand for advanced energy-saving technologies has increased with the increasingly stringent vehicle emission standards and rising energy costs in every country [1]. Loaders have a wide range of applications and are one of the primary construction vehicles, with significant ownership [2,3]. In the operation process of frequently loading and unloading materials, the boom cylinder of loaders performs a series of periodic and repetitive actions. A large amount of boom arm potential energy is converted into thermal energy through a multi-way valve [4]. This results in a significant rise in hydraulic oil temperature, which directly deteriorates the regular operation of the loader in severe cases. Therefore, the energy recovery and regeneration of the potential energy of the loader boom arm can not only effectively solve the problem of the rapid rise in hydraulic oil temperature but can also reduce the fuel consumption of the loader engine.

Energy recovery can be divided into mechanical, electrical, and hydraulic types [5,6] for hydraulic systems. The mechanical types are further subdivided into the flywheel, counterweight, and spring types [7]. Flywheel types mainly use a rotating flywheel as an energy storage element, which has the advantages of high efficiency, fast response time, long life, and the easy monitoring of energy storage status [8]. The electrical types use

supercapacitors or batteries as energy storage elements. The hydraulic motors drive the generator to generate electricity, converting the hydraulic energy that the system needs to recover into electricity. The energy is then stored and regenerated through an electrical energy storage system with high energy recovery efficiency [9]. Hydraulic types use accumulators as energy storage elements. Compared to mechanical and electrical types, hydraulic types have fewer conversion links, lower costs, and higher reliability [10]. It is more suitable for construction machinery in harsh working environments [11].

Research on the energy recovery and regeneration of hydraulic systems and the optimization of hybrid system parameters has been the focus of scholars [12–15]. Xiangyun Shi combined the loader system configuration and working condition characteristics with the building of a forward simulation model. Furthermore, the typical actuator of the loader was developed, and the building process was described. She used the forward simulation model and demonstrated the rationality of the energy management strategies for serial and parallel oil–hydraulic hybrids [16]. Hui S proposed a parallel hydraulic hybrid power saving system, combining the actuator’s characteristics of the loader. This hydraulic energy-saving system’s brake energy recovery and energy regeneration control strategy were developed, i.e., auxiliary power output in high load conditions and the recovery of loader braking energy in low and medium braking intensity conditions [17]. Dandan Zhang addressed the shortcomings of the current parallel hydraulic hybrid vehicles which cannot combine braking performance and energy recovery performance. The AMESim-based dual-accumulator hydraulic hybrid vehicle and its control strategy model were established using a dual-accumulator-by-accumulator liquid-filling scheme. Furthermore, the simulation analysis study was conducted under the vehicle’s high and low-speed braking conditions [18]. TianLiang Lin proposed an excavator arm energy recovery system using a proportional throttle valve and a solenoid-proportional reversing valve. Experimental research showed that the recovery efficiency of this energy recovery system was about 35% [19].

Optimizing the hydraulic system can effectively improve the functional performance of the hydraulic system [20,21]. For the hybrid hydraulic energy recovery system, the parameters of hydraulic components directly affect the energy-saving effect of the system. The influence law of component parameters on system energy-saving can be obtained through the optimization analysis of hydraulic component parameters. Reasonable parameter setting according to the law can effectively improve the energy-saving effect of the system. When the parameter optimization analysis of hydraulic components is carried out, the equipment installation requirements, component economy, and model must be considered. The research proposes a hybrid loader boom arm energy recovery and regeneration system based on the above analysis. The system uses an accumulator as the energy storage element.

This paper is organized as follows. Section 2 introduces the principle of energy recovery and regeneration system of the hybrid loader actuator. Section 3 introduces the mathematical model analysis of hydraulic components. Section 4 introduces the system modeling and simulation. Section 5 introduces the system simulation results analysis. Section 6 introduces the system component parameter optimization analysis. Section 7 introduces the system energy-saving analysis. Section 8 is the conclusion.

## **2. Principle of Energy Recovery and Regeneration System of the Hybrid Loader Actuator**

At present, the energy loss of the hydraulic system of the loader actuator is mainly divided into throttling loss and overflow loss. The throttling loss is mainly the energy loss caused by the pressure drop through the multi-way valve, and this part of energy loss is challenging to avoid. The overflow loss is the energy loss caused by the mismatch between the flow rate of pump output and the flow rate of load demand, resulting in the overflow of excess flow through the relief valve. The problem can be effectively solved by using load-sensing technology. Therefore, this technology is widely used in loaders.



### 2.1. Hydraulic System Principle of Loader Actuator

Figure 1 shows the hydraulic system schematic diagram of the loader actuator. The system consists of a boom subcircuit and a bucket subcircuit. Shuttle valve 7 feeds back the maximum pressure of each subcircuit to load-sensing pump 1. Load-sensing pump 1 supplies boom cylinders 12.1 and 12.2, and bucket cylinder 11. Due to the use of pre-valve pressure compensation technology in both branches, i.e., pressure compensation, valves 7.1 and 7.2 are respectively in a series in front of the main valves 10 and 9, cylinders 12.1 and 12.2, and cylinder 11 can perform combined actions. Safety valve 4 has overload protection. One-way relief valves 13.1, 13.2, and 13.3 have overload protection and oil-filling functions. The pilot pressure controller 16 guarantees a stable pilot pressure in the pilot circuit.

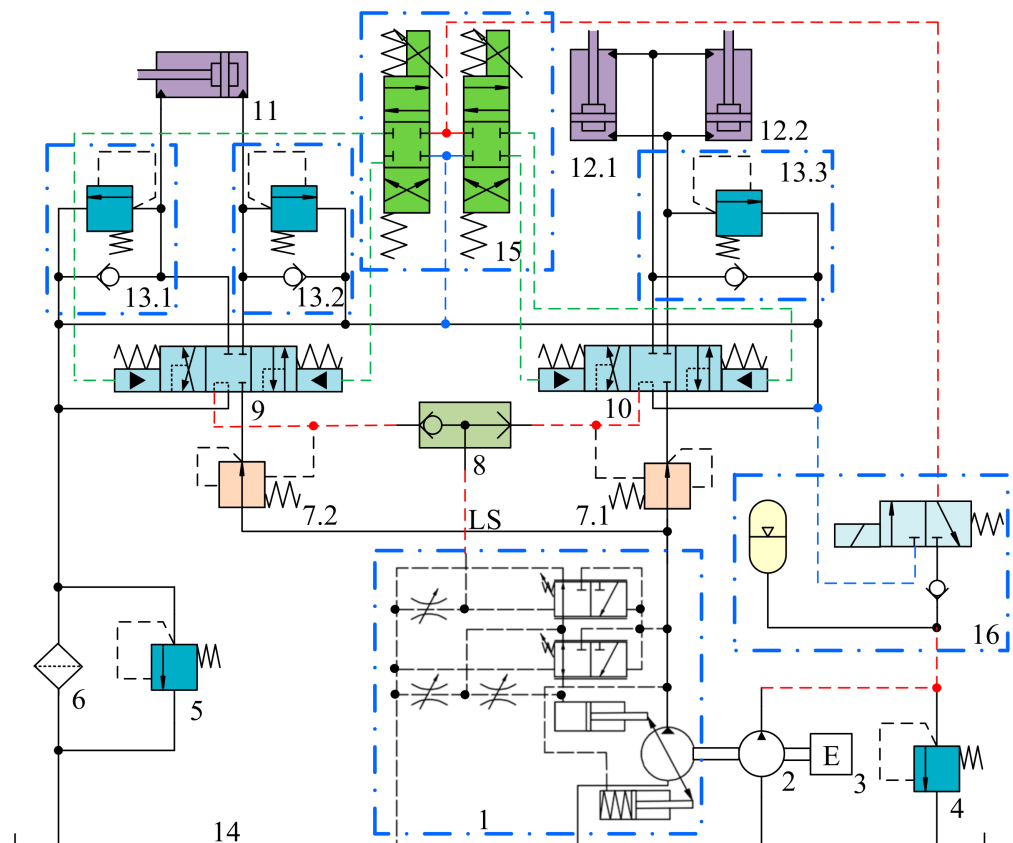


**Figure 1.** Hydraulic system schematic diagram of loader actuator. 1. Load-sensing pump. 2. Auxiliary pump. 3. Engine. 4. Safety valve. 5. Relief valve. 6. Filter. 7.1~7.2. Pressure compensation valve. 8. Shuttle valve. 9. Main valve of bucket multi-way valve. 10. Main valve of boom multi-way valve. 11. Bucket cylinder. 12.1~12.2. Boom cylinder. 13.1~13.3. One-way relief valve. 14. Tank. 15. Pilot valve. 16. Pilot pressure controller.

### 2.2. Principle of Energy Recovery and Regeneration System for Hybrid Loader Actuator

Figure 2 shows the schematic diagram of hybrid loader actuators' energy recovery and regenerative hydraulic system. The system consists of the loader actuator hydraulic and the hydraulic energy recovery and regeneration system. Figure 3 shows the system energy recovery and regeneration control strategy diagram. The control strategy is based on the boom cylinder control signal. When the boom arm drops, the system enters energy recovery mode. Valves 16 and 17.1 work in the right position, and valve 17.2 works in the left position. Accumulator 19 is charged. Accumulator 19 recovers energy, and the system is driven by engine 3. When the working pressure of accumulator 19 is over the set maximum working pressure, valve 16 works in the left position, and valves 17.1 and 17.2 work in the right position. Accumulator 19 stops charging, and the system stops

energy recovery. Otherwise, energy recovery continues. When the boom arm rises, the system enters the energy regeneration mode. Valves 16, 17.1, and 17.2 work in the left position. Accumulator 19 releases energy, and the system is driven by engine 3 and energy regeneration hydraulic motor 18. When the working pressure of accumulator 19 is lower than the set minimum pressure, valve 16 works in the left position and valves 17.1 and 17.2 work in the right position. Accumulator 19 stops discharging, i.e., the system stops energy regeneration. Otherwise, continue to regenerate energy. When the boom cylinder is stationary, valve 16 works in the left position and valves 17.1 and 17.2 work in the right position. Accumulator 19 is not charged and discharged. Accumulator 19 does not perform the recovery and release of energy, and the system is driven by engine 3.

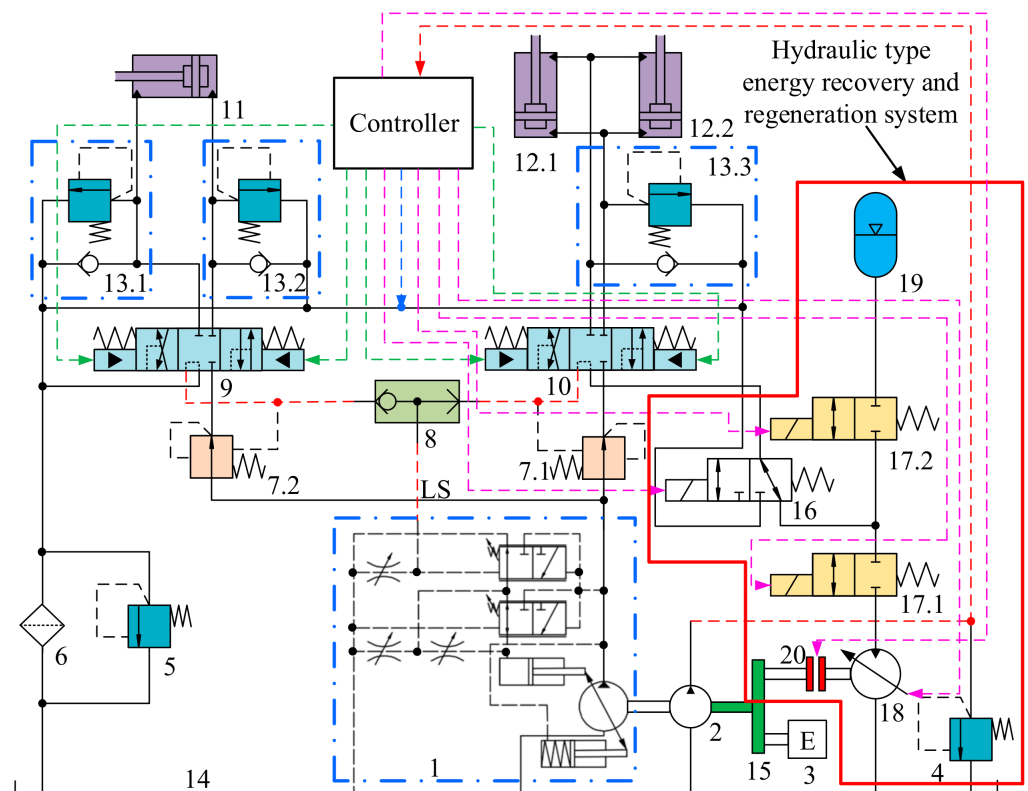


**Figure 2.** Schematic diagram of hybrid loader actuators' energy recovery and regenerative hydraulic system. 1. Load-sensing pump. 2. Auxiliary pump. 3. Engine. 4. Safety valve. 5. Relief valve. 6. Filter. 7.1~7.2. Pressure compensation valves. 8. Shuttle valve. 9. Main valve of bucket multi-way valve. 10. Main valve of boom multi-way valve. 11. Bucket cylinder. 12.1~12.2. Boom cylinder. 13.1~13.3. One-way relief valve. 14. Tank. 15. Torque coupler. 16. Two positions three-way solenoid directional valve. 17.1~17.2. Two positions two-way solenoid directional valve. 18. Energy regeneration hydraulic motor. 19. Accumulator. 20. Clutch.

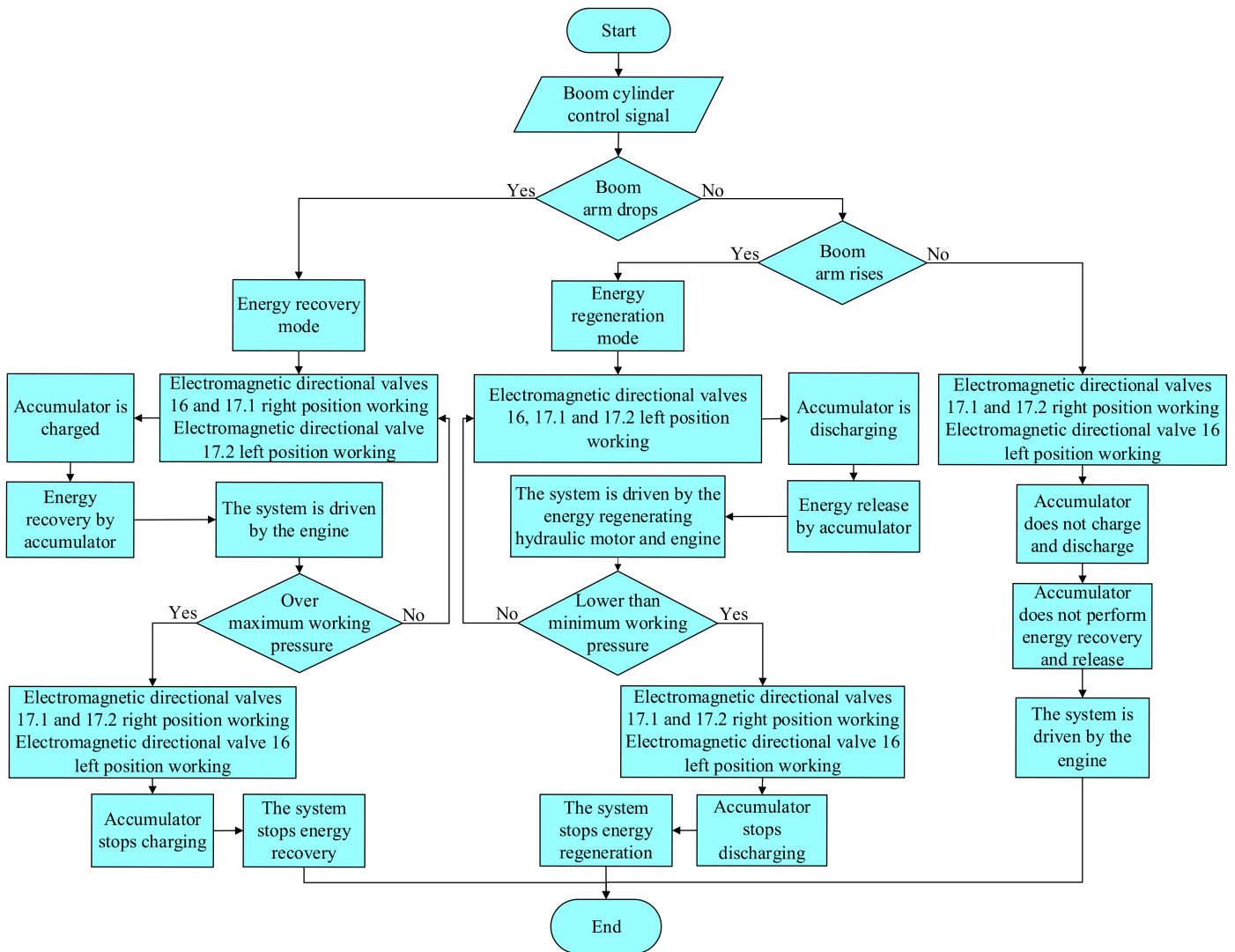


Figure 3. System energy recovery and regeneration control strategy diagram.

### 3. Mathematical Model Analysis of Hydraulic Components

#### 3.1. Mathematical Model Analysis of Engine

The engine is Weifang Steyr WD10G220E2, and the engine efficiency is 35~45%. When the engine torque and speed are determined, the fuel consumption rate at a certain speed and torque is determined by checking the table [2]. The engine fuel consumption [2] can be described as:

$$m_u = \int \frac{T_c n_c f_u(T_c, n_c)}{9550 \times 3600} dt \quad (1)$$

where  $m_u$  is the engine fuel consumption, g;  $T_c$  is the engine torque, N·m;  $n_c$  is the engine speed, rev/min;  $f_u(T_c, n_c)$  is the engine fuel consumption rate, g/kW·h.

The engine efficiency can be described as:

$$\eta_e = \frac{W_e}{Q_e} \quad (2)$$

where  $\eta_e$  is the engine efficiency;  $W_e$  is the useful work conducted by the engine, kJ;  $Q_e$  is the energy released by fuel combustion, kJ.

### 3.2. Mathematical Model Analysis of Boom Cylinder

When the boom arm drops, a large amount of boom potential energy is converted into pressure energy through the piston side of the boom cylinder. Therefore, the energy flowing out of the piston side of the boom cylinder can be used as the recoverable energy of the boom cylinder. Then the recoverable energy of the boom cylinder [22] can be described as:

$$E_1 = \frac{1}{1000} \int p \times Q dt \quad (3)$$

where  $E_1$  is the recoverable energy of the boom cylinder, kJ;  $p$  is the pressure of the piston side of the boom cylinder when the boom drops, Pa;  $Q$  is the flow rate of the piston side of the boom cylinder when the boom arm drops,  $\text{m}^3/\text{s}$ .

### 3.3. Mathematical Model Analysis of Accumulator

The accumulator recovers and stores the recoverable energy of the boom cylinder. The airbag accumulator is used in the research. The gas in the accumulator airbag is usually inert, as with the ideal gas volume. According to Boyle's law [23]:

$$p_1 V_1^n = p_2 V_2^n = \text{const} \quad (4)$$

where  $p_1$  is the minimum working pressure, Pa;  $V_1$  is the volume corresponding to the minimum working pressure,  $\text{m}^3$ ;  $p_2$  is the maximum working pressure, Pa;  $V_2$  is the volume corresponding to the maximum working pressure,  $\text{m}^3$ ;  $n$  is the polytropic index of gas under adiabatic condition, which is 1.4.

The principle of energy recovery and energy release of the accumulator is the same. Therefore, according to Equation (4), the energy recovered by the accumulator [23] can be described as:

$$E_2 = \frac{1}{1000} \int_{V_3}^{V_4} p_d dV = \frac{1}{10} \times \frac{p_4 V_4}{n-1} \left[ \left( \frac{p_3}{p_4} \right)^{\frac{n-1}{n}} - 1 \right] \quad (5)$$

where  $E_2$  is energy recovered by the accumulator, kJ;  $V_4$  is the volume of accumulator before storing energy,  $\text{m}^3$ ;  $V_3$  is the volume after energy storage of accumulator,  $\text{m}^3$ ;  $p_d$  is the pressure of energy storage process of the accumulator, Pa;  $p_4$  is the pressure before energy storage of accumulator, Pa;  $p_3$  is the pressure after energy storage of accumulator, Pa.

The accumulator energy density [23] can be described as:

$$E_v = \frac{p_1}{1-n} \left[ 1 - \left( \frac{p_1}{p_2} \right)^{\frac{1-n}{n}} \right] \quad (6)$$

where  $E_v$  is the accumulator energy density.

Because the energy density of the accumulator is low, the larger the energy density per unit volume, the better. When  $E_v$  reaches the maximum value, i.e., the accumulator can achieve maximum energy recovery efficiency in the limited installation space of the loader. When  $\frac{dE_v}{dp_1} = 0$ ,  $E_v$  reaches the maximum value [24,25].

When the boom arm drops, the pressure in the piston side of the boom cylinder increases with the working pressure of the accumulator increasing. If the working pressure of the accumulator is too high, it will affect the boom cylinder's movement characteristics and the system's energy recovery efficiency. Based on the above analysis, we combined the pressure of the piston side of the boom cylinder. When the boom arm drops in the conventional system,  $p_2 < 52$  bar. In order to prevent the airbag of the accumulator from being too much and damaging the airbag, the inflation pressure of the accumulator should not be too enormous. At the same time, to reduce the accumulator's mass, the filling pressure of the accumulator should not be too small. Therefore, the accumulator filling pressure [26] can be described as:

$$0.25p_2 \leq p_0 \leq 0.9p_1 \quad (7)$$

where  $p_0$  is the accumulator filling pressure.

Based on the analysis of Equation (7) above, the accumulator pressure is preliminarily set as  $p_0 = 13$  bar,  $p_1 = 26$  bar,  $p_2 = 50$  bar.

During the boom arm dropping process, the accumulator recovers the oil in the piston side of the boom cylinder. Then the volume of oil flowing out the piston side of the boom cylinder is equal to the volume of oil recovered by the accumulator. Then the rated volume of the accumulator [26] can be described as:

$$V_0 = \Delta V \frac{\left(\frac{p_1}{p_0}\right)^{\frac{1}{n}}}{1 - \left(\frac{p_1}{p_2}\right)^{\frac{1}{n}}} \quad (8)$$

where  $V_0$  is the rated volume of the accumulator, L;  $\Delta V$  is the volume of oil recovered by the accumulator, L.

When the rated volume of the accumulator increases, the accumulator's cost increases. At the same time, considering the loader's installation size limitation, the accumulator's rated volume cannot be too large. Based on the analysis of Equation (8) above and combined with the following parameters, the rated volume of the accumulator is preliminarily set as  $V_0 = 55$  L.

### 3.4. Mathematical Model Analysis of Energy Regeneration Hydraulic Motor

When the boom arm rises, the hydraulic motor converts the pressure energy stored in the accumulator into mechanical energy. The displacement of the hydraulic motor is mainly considered. According to the maximum velocity of the boom cylinder, the diameter of the piston side of the boom cylinder, and the maximum speed of the torque coupler, the displacement of the hydraulic motor [22] can be described as:

$$q = \frac{\pi d^2 v_{bmax}}{4n_{amax}} \quad (9)$$

where  $q$  is the displacement of the hydraulic motor,  $m^3/\text{rev}$ ;  $d$  is the diameter of the piston side of the boom cylinder, m;  $v_{bmax}$  is the maximum velocity of boom cylinder, m/s;  $n_{amax}$  is the maximum speed of the torque coupler, rev/s.

When the displacement of the hydraulic motor is too large, the volume, quality, and cost of the hydraulic motor increase at the same time; considering the loader's installation size limitation, the hydraulic motor's displacement should not be too large. Based on the analysis of Equation (9) above and combined with the following parameters, the hydraulic motor displacement is preliminarily set as  $q = 90$  mL/rev.

## 4. System Modeling and Simulation

The hybrid system consists of the load-sensing pump, energy recovery and regeneration system, engine system, etc. The load-sensing pump, actuator, multi-way valve, and system model are analyzed below.

### 4.1. Load-Sensing Pump Modeling

The load-sensing pump is a Rexroth A10VSO series variable pump, and the total efficiency of this series of load-sensing pump is 80% to 90%. Figure 4 shows the load-sensing pump schematic. The load-sensing pump consists of a load-sensing valve, a pressure shut-off valve, and a plunger cylinder. Load-sensing pumps control the pump outlet pressure according to the force on both sides of the load-sensing valve and pressure shut-off valve under different external loads. When the load-sensing valve and pressure shut-off valve operate, the piston movement of the plunger cylinder is controlled at the same time. It controls the swashplate tilt angle of the load-sensing pump and enables the system to output the flow required by the load.



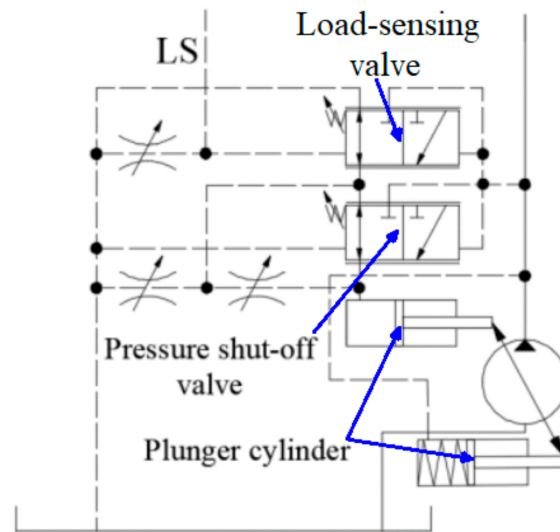


**Figure 4.** Load-sensing pump schematic.

According to Newton's second law, the load-sensing valve spool mechanical equilibrium equation [27] can be described as:

$$(p_b - p_L - p_d)A_v - K_{LS}x_{LS} = M_v \frac{d^2 x_{LS}}{dt^2} \quad (10)$$

where  $p_b$  is the pump outlet pressure, Pa;  $p_L$  is the load pressure, Pa;  $p_d$  is the preset pressure, Pa;  $A_v$  is the spool force area,  $m^2$ ;  $K_{LS}$  is the spring stiffness;  $x_{LS}$  is the spool displacement, m;  $M_v$  is the spool mass, kg.

According to the flow continuity principle, the flow through the damped orifice in the load-sensing valve [27] can be described as:

$$Q_{LS} = C_d w x_{LS} \sqrt{\frac{2\Delta p_{LS}}{\rho}} \quad (11)$$

where  $Q_{LS}$  is the flow rate through the load-sensing valve,  $m^3/s$ ;  $C_d$  is the flow coefficient;  $w$  is the spool area gradient;  $\Delta p_{LS}$  is the pressure difference before and after the load-sensing valve, Pa;  $\rho$  is the oil density,  $kg/m^3$ .

The opening area of the load-sensing valve is proportional to the product of the area gradient and displacement, with the direction of increasing the spool opening area of the load-sensing valve being positive. Then the flow gain and pressure gain of the load-sensing valve [27] can be described as:

$$\left\{ \begin{array}{l} K_q = \frac{\partial Q_{LS}(s)}{\partial x_{LS}} = C_d w \sqrt{\frac{2(p_b - p_5)}{\rho}}, (x_{LS} \geq 0) \\ K_q = C_d w \sqrt{\frac{2p_6}{\rho}}, (x_{LS} \leq 0) \\ K_p = -\frac{\partial Q_{LS}(s)}{\partial p} = \frac{C_d w x_{LS}}{\sqrt{2(p_b - p_5)\rho}}, (x_{LS} \geq 0) \\ K_p = \frac{C_d w x_{LS}}{\sqrt{2p_6\rho}}, (x_{LS} \leq 0) \end{array} \right. \quad (12)$$

where  $K_q$  is the flow gain;  $K_p$  is the pressure gain;  $p_5$  is the piston side of the plunger cylinder pressure when the pump outlet flow rate reduces, Pa;  $p_6$  is the piston side of the plunger cylinder when the pump outlet flow rate increases, Pa.

The load-sensing pump regulates the pump outlet flow by adjusting the swashplate tilt angle through the plunger cylinder. Considering the oil's elastic modulus, pressure

leakage coefficient, and output efficiency, from the flow continuity principle, the pump outlet flow rate [27] can be described as:

$$Q_p = K_q x_{LS} \eta_v = \left[ A_1 \frac{dx_p}{dt} + \frac{VJd^3x_p}{\beta A_1 r_0^2 dt^3} + (K_p + c_0) \frac{Jd^2x_p}{A_1 r_0^2 dt^2} \right] \eta_v \quad (13)$$

where  $Q_p$  is the pump outlet flow rate,  $m^3/s$ ;  $A_1$  is the area of the piston side of the plunger cylinder,  $m^2$ ;  $V$  is the pump displacement,  $m^3/rev$ ;  $J$  is the load-sensing pump rotational inertia,  $kg.m^2$ ;  $x_p$  is the plunger cylinder displacement,  $m$ ;  $\beta$  is the hydraulic elastic modulus of elasticity,  $Pa$ ;  $r_0$  is the distance between plunger disc and piston rod mid-axis,  $m$ ;  $c_0$  is the leakage coefficient;  $\eta_v$  is the volumetric efficiency.

The total efficiency of the load-sensing pump [27] can be described as:

$$\eta = \eta_v \cdot \eta_m \quad (14)$$

where  $\eta$  is the total efficiency of the load-sensing pump;  $\eta_m$  is the mechanical efficiency of the load-sensing pump.

Based on the above Equations (10)–(13), the AMESim HCD library and the hydraulic library are used to build the model shown in Figure 5. Where the proportional throttle simulates the load flow demand, the proportional relief valve simulates load pressure changes. The load-sensing pump parameters are set as shown in Table 1. The proportional throttle pressure flow curves are shown in Figure 6. When the load pressure changes, the load-sensing pump outlet pressure changes. The proportional throttle valve has a constant differential pressure of 15 bar before and after the valve.

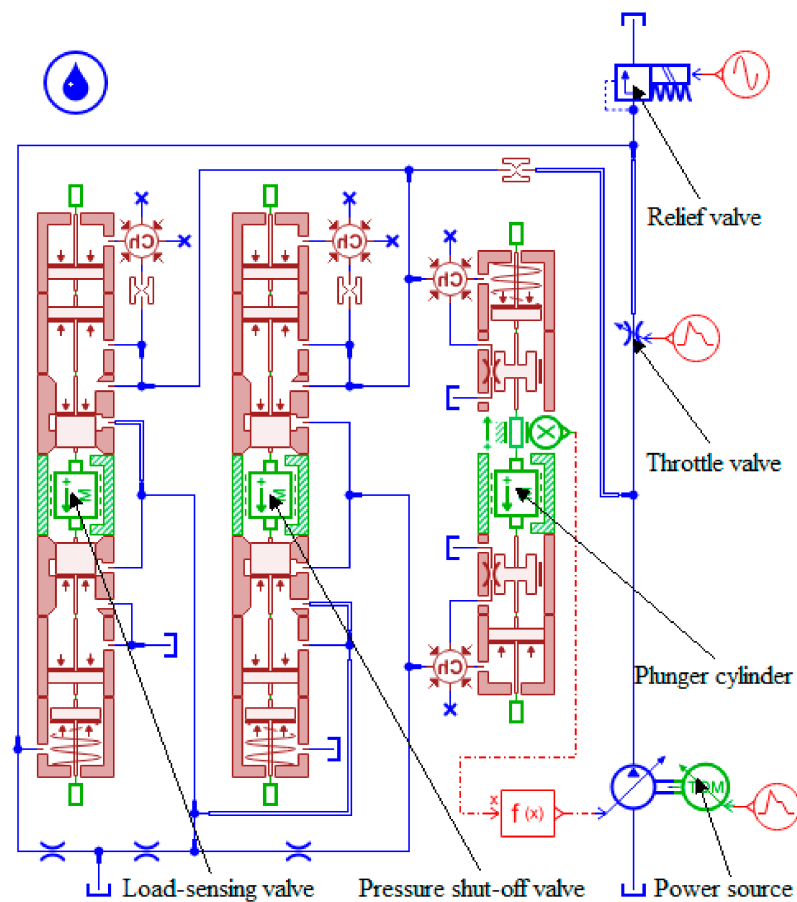
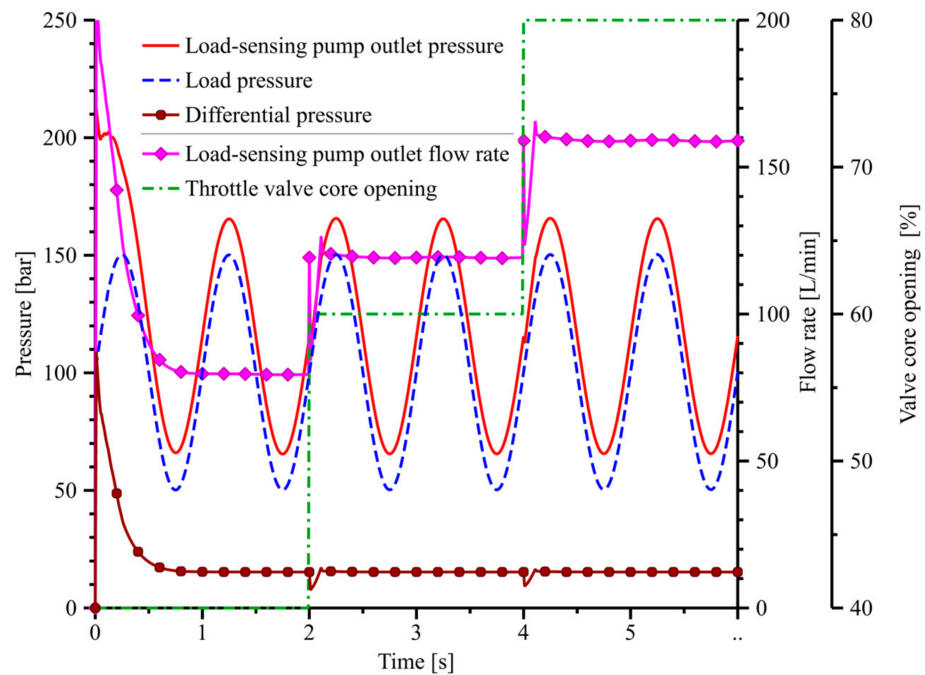


Figure 5. Load-sensing pump simulation model.

**Table 1.** Load-sensing pump parameters.

Parameters	Value
Load-sensing valve preset differential pressure	15 bar
Pressure cut-off valve pressure	170 bar
Maximum opening area diameter of the proportional throttle	0.01 m
Displacement	200 mL/rev
Power source speed	2000 rev/min



**Figure 6.** Proportional throttle pressure flow curves.

As mentioned above, the flow rate required by the system’s load is independent of the load pressure and proportional to the opening area of the proportional throttle valve. It implements the primary function of the load-sensing pump in preparation for subsequent research.

*4.2. Actuator Modeling*

The research object of the paper is a 50-type wheel loader. It is a Chinese loader model with a rated load of 5 t, according to the two-dimensional drawings acquired from the manufacturer to obtain the specific dimensions of each component and the location of the articulated point between the cylinder and the frame [26]. The parameters of the actuator are shown in Table 2. The AMESim 2D mechanical library is used to build the loader actuator simulation model, as shown in Figure 7, for subsequent research.

**Table 2.** Actuators parameters.

Parameters	Mass	Horizontal Distance from Front Wheel Center	Vertical Distance from the Center of the Front Wheel
Bucket center	—	1.849 m	0.3187 m
Boom arm	1219.1 kg	0.531 m	0.6138 m
Rocker arm	285.9 kg	0.9766 m	0.6301 m
Rotary bucket	1433.8 kg	1.843 m	0.1038 m
Pull rod	43 kg	0.864 m	−0.0591 m

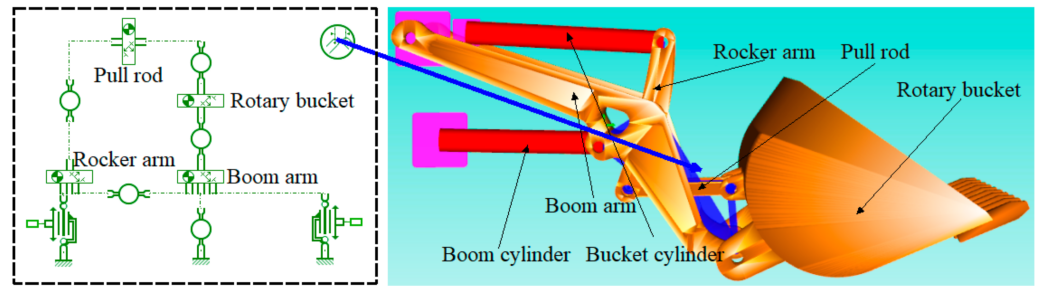


Figure 7. Simulation model of the actuator.

#### 4.3. Multi-Way Valve Modeling

The multi-way valve in the research adopts a pilot-operated electro-hydraulic proportional directional valve, which consists of the main and pilot valve. By adjusting the size of the current signal of the pilot valve proportional solenoid, the displacement size of the pilot valve spool is adjusted, controls the flow into both ends of the main valve spool, and regulates the displacement of the main valve spool. The pilot valve’s proportional solenoid input current signal is proportional to the main valve spool displacement, thus realizing the hydraulic actuator speed adjustment. Since the pilot valve and the main valve control flow principle are the same, the main valve is analyzed as an example.

According to Newton’s second law, the equation of mechanical equilibrium of the main spool of the multi-way valve [26] can be described as:

$$F_e - F_0 = M_m \frac{d^2x_m}{dt^2} + B_m \frac{dx_m}{dt} + K_S x_m \tag{15}$$

where  $F_e$  is the hydraulic pilot force on one side of the main valve spool, N;  $F_0$  is the hydraulic pilot force on the other side of the main valve spool, N;  $M_m$  is the main valve spool mass, kg;  $x_m$  is the main valve spool displacement, m;  $B_m$  is the viscous damping coefficient;  $K_S$  is the main valve spring stiffness.

According to the flow continuity principle, the flow rate of the main spool of the multiway valve [26] can be described as:

$$Q_m = C_d w_m x_m \sqrt{\frac{2(p_p - p_L)}{\rho}} \tag{16}$$

where  $Q_m$  is the flow rate through the main valve spool, m<sup>3</sup>/s;  $C_d$  is the flow coefficient;  $w_m$  is the spool area gradient;  $p_p$  is the pump outlet pressure, Pa;  $p_L$  is the load pressure, Pa.

Based on the analysis of Equations (15) and (16), the AMESim HCD library is used to build the model shown in Figure 8. The multi-way valve parameters are set as shown in Table 3 for the subsequent research.

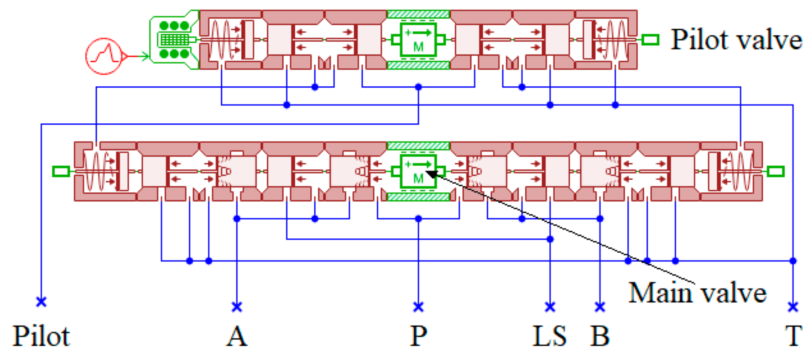


Figure 8. Multi-way valve simulation model.

**Table 3.** Multi-way valve parameters.

Parameters	Value
Pilot valve spool diameter	0.0025 m
Main valve spool diameter	0.01 m
Maximum spool displacement of pilot valve	0.00025 m
Maximum spool displacement of main valve	0.0005 m
Pilot valve spool mass	0.01 kg
Main valve spool mass	0.05 kg
Proportional solenoid rated current	100 mA
Damping factor	50 N/(m/s)

#### 4.4. System Modeling

Based on the above Sections 4.1–4.3 analyses, combined with Section 2.2, AMESim is used to build the simulation model, as shown in Figure 9. In order to improve the accuracy of cylinder position control and the stability of the whole actuator [15], a position control system using a PID controller control has been designed.

Loaders can perform shoveling operations and short-distance material transportation. Among them, the flexible combination of shovel operation and dump truck can have a variety of operations [25]. The I-type working condition [26] is one of the most common ways of working when conducting loader experiments due to the higher number of operations per unit. Only the loader actuator system is considered in this research. Since the loader is usually unloaded when the boom arm drops, the weight of the material is not considered in this simulation. Combined with the above analyses, the I-type working condition is used as a typical working condition.

The cylinder control signal is set as shown in Figure 10. The system completes a complete typical working condition in 25 s. According to the displacement set by the boom and bucket cylinders, the system completes the excavation action between 0 and 5 s. The system completes the raising action between 5 s and 11 s. The system completes dumping action between 11 s and 17 s. The system completes the resetting between 17 s and 25 s. The system simulation time is set to 75 s, i.e., three working actions are completed in typical working conditions. Combining the above Sections 3.3 and 3.4 analyses and the information provided by the 50-type wheel loader manufacturer, the system simulation parameters are set, as shown in Table 4.

**Table 4.** Key component parameters.

Components	Parameters	Value
Engine	Rated speed	2000 rev/min
	Specific heat value of fuel	42700 kJ/kg
	Number of cylinders	6
Boom cylinder	Piston diameter	0.165 m
	Rod diameter	0.08 m
	Stroke length	0.757 m
Bucket cylinder	Piston diameter	0.2 m
	Rod diameter	0.1 m
	Stroke length	0.54 m
Pressure compensation valve	Preset differential pressure	10 bar
Accumulator	Initial filling pressure	13 bar
	Maximum working pressure	50 bar
	Initial rated volume	55 L
Energy regeneration hydraulic motor	Initial displacement	90 mL/rev
	Efficiency	80~90%



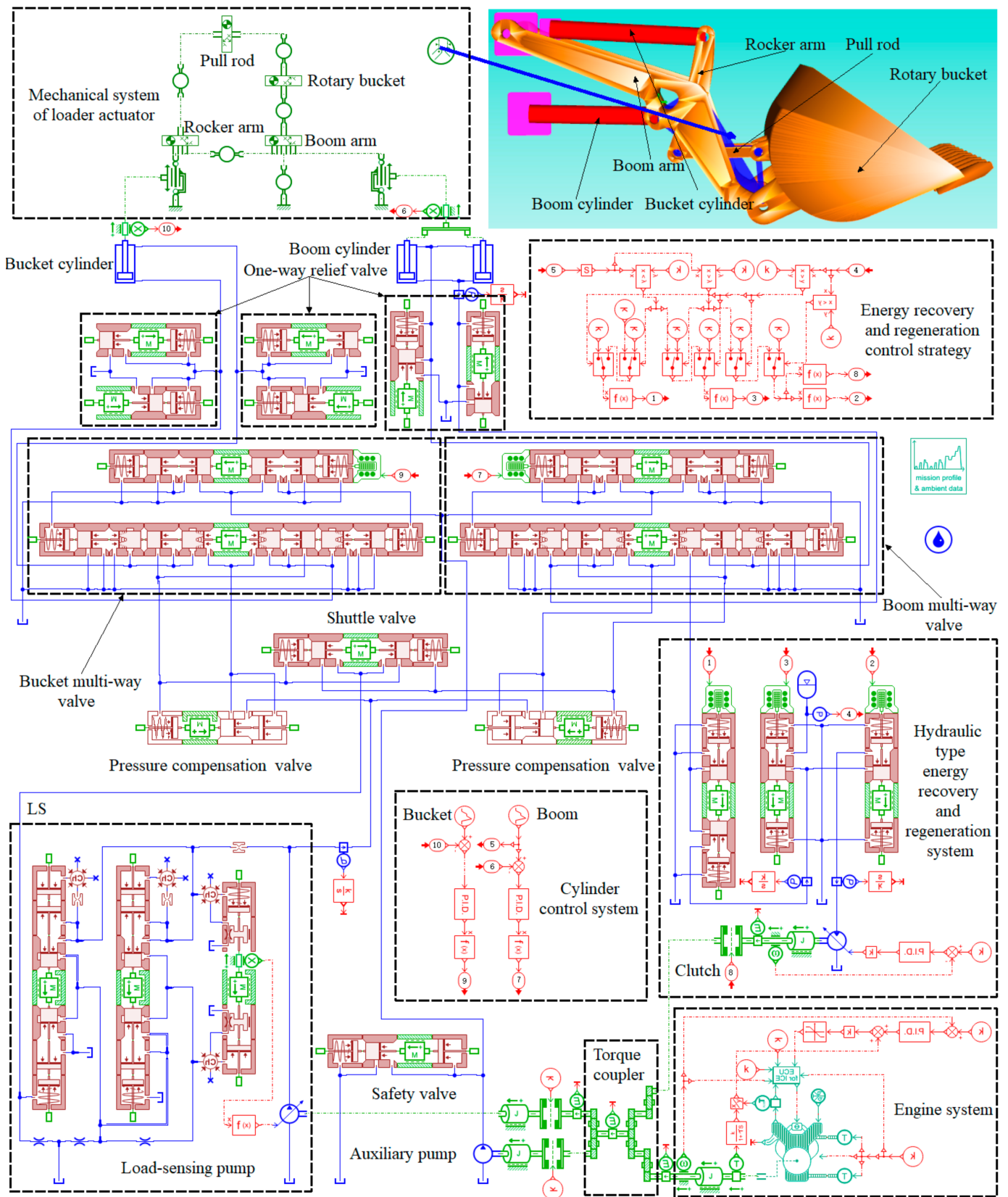


Figure 9. System simulation model.

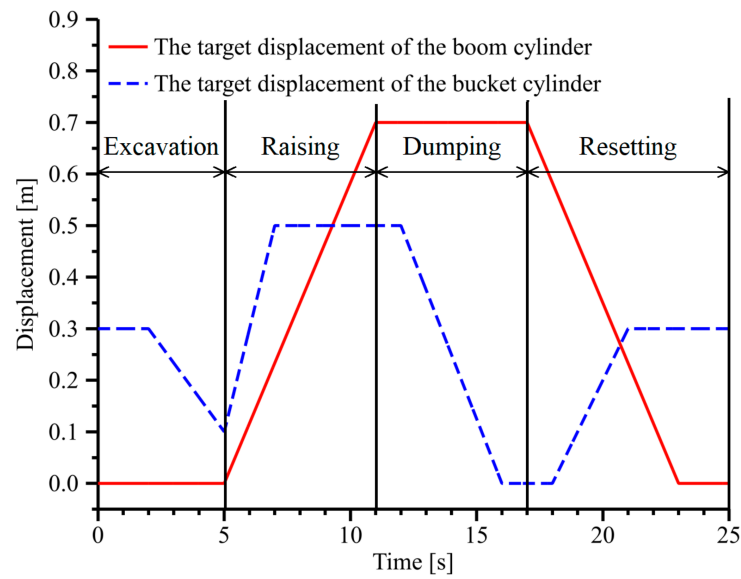


Figure 10. Cylinder control signal curves.

### 5. System Simulation Results Analysis

#### 5.1. Cylinder Motivation Characteristics Analysis

Figure 11 shows the cylinder displacement curves. Figure 12 shows the cylinder velocity curves. Since the system adopts the PID controller for feedback control, the boom and bucket cylinder displacement and velocity can better track the boom and bucket cylinder's target displacement and velocity. When the boom cylinder and bucket cylinder's target displacement and velocity change, the boom cylinder and the bucket cylinder's displacement and velocity fluctuate less. In summary, the hybrid system actuator is responsive and can meet the regular operation needs of the loader.

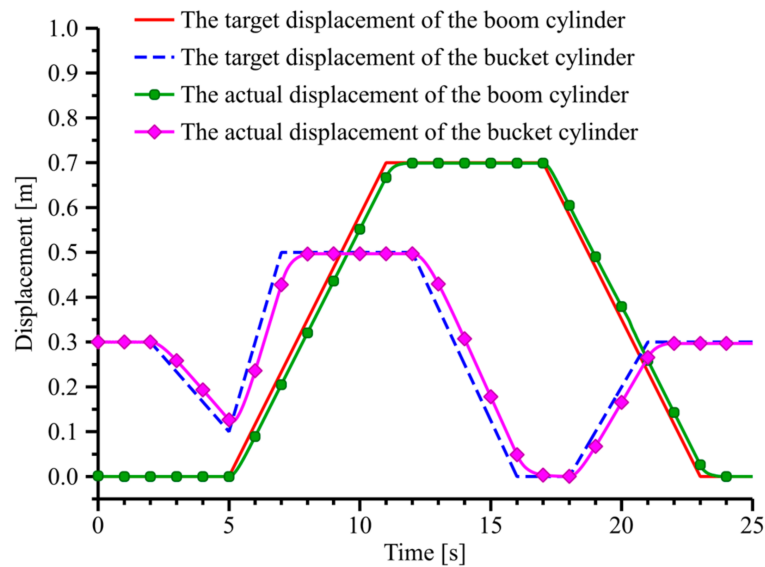


Figure 11. Cylinder displacement curves.

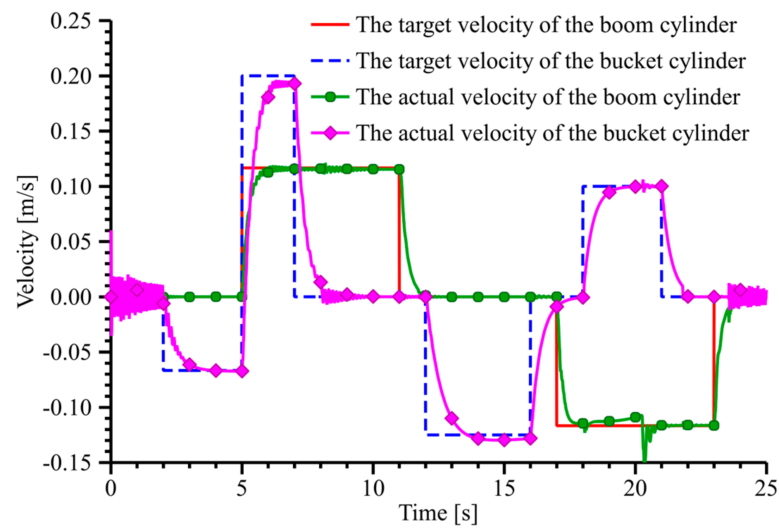


Figure 12. Cylinder velocity curves.

### 5.2. System Energy Recovery and Regeneration Analysis

Figure 13 shows the accumulator gas pressure, volume, and power curves. The system performs energy regeneration between 5 s and 11 s. The accumulator gas pressure reduces from 40.6 bar to 13 bar. The accumulator gas fill percentage increases from 45% to 99.8%. The accumulator discharging power reduces from 18.7 kW to 6.8 kW. The system performs energy recovery between 17 s and 23 s. The accumulator gas pressure increases from 13 bar to 40.8 bar. The accumulator gas fill percentage reduces from 99.8% to 44.9%. The accumulator charges power increases from 7.1 kW to 20 kW.

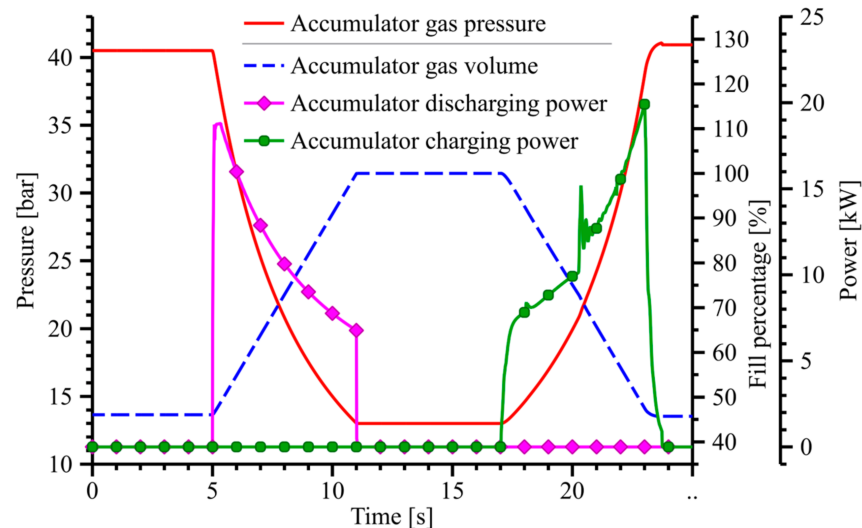
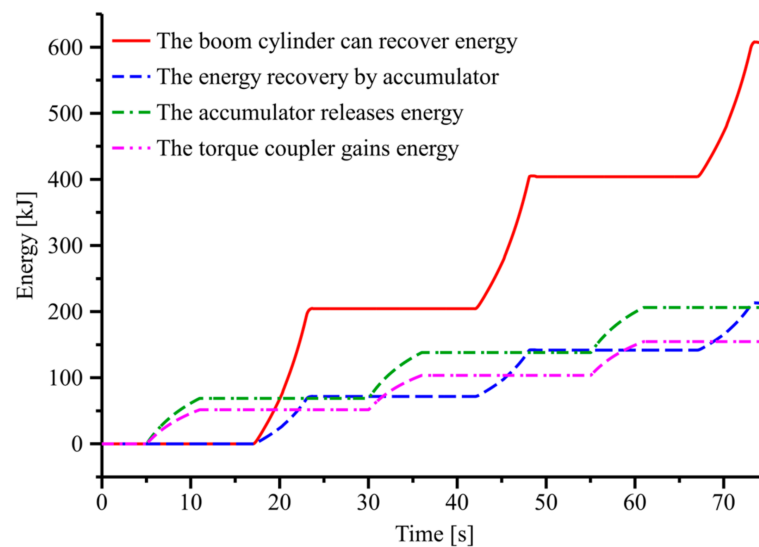


Figure 13. Accumulator gas pressure, volume and power curves.

The system energy recovery and regeneration curves can be obtained from Equations (3) and (5) combined with the system simulation model, as shown in Figure 14. The total recoverable energy of the boom cylinder is 610.2 kJ, the total recover energy of the accumulator is 216.7 kJ, and the energy recovery efficiency of the system is 35.5%. The total energy released by the accumulator is 210.4 kJ, the total energy gained by the torque coupler is 156.5 kJ, and the energy regeneration efficiency is 74.4%.



**Figure 14.** System energy recovery and regeneration curves.

In summary, the hybrid system accumulator pressure and volume can be restored to the initial set filling pressure and rated volume, ensuring the system's continuous energy recovery and regeneration action. The hybrid system has low energy recovery and regeneration efficiency, and the parameters can be optimized to improve the system's energy recovery and energy regeneration efficiency.

## 6. System Component Parameter Optimization Analysis

Since the accumulator recovers the energy, the energy regeneration hydraulic motor regenerates the energy for this hybrid system. Therefore, when the energy recovery efficiency and the energy regeneration efficiency reach the maximum, the energy-saving effect of the system is at its best. This research uses the optimization objective of maximum energy recovery and energy regeneration efficiency. It analyzes the influence of the accumulator and the energy regeneration hydraulic motor parameters on the system's energy recovery and energy regeneration efficiency. The system's energy-saving effect is analyzed with the accumulator's actual model.

### 6.1. Parameter Optimization Analysis of Accumulator and Energy Regeneration Hydraulic Motor

As the energy storage and energy regeneration components of the hybrid system, the advantages and disadvantages of the parameters of the accumulator and the energy regeneration hydraulic motor directly affect the functional performance of the hybrid system. Therefore, we analyze the effect of accumulator filling pressure and rated volume on energy recovery efficiency and the effect of energy regeneration hydraulic motor displacement on energy regeneration efficiency.

#### 6.1.1. Analysis of the Effect of the Filling Pressure of the Accumulator on Energy Recovery

Based on the simulation model and combined with Equation (6), keeping other system parameters constant. The accumulator filling pressure is set to 12.5 bar to 30 bar, and the system energy recovery efficiency is analyzed under the rated volume of the accumulator at 45 L, 55 L, and 65 L. Figure 15 shows the accumulator variable filling pressure energy recovery efficiency curves. The energy recovery efficiency of the system shows a rising and then decreasing trend as the accumulator filling pressure rises. As the volume of the accumulator increases, the system energy recovery efficiency gradually increases. Therefore, the system can improve energy recovery efficiency by increasing the accumulator filling pressure.

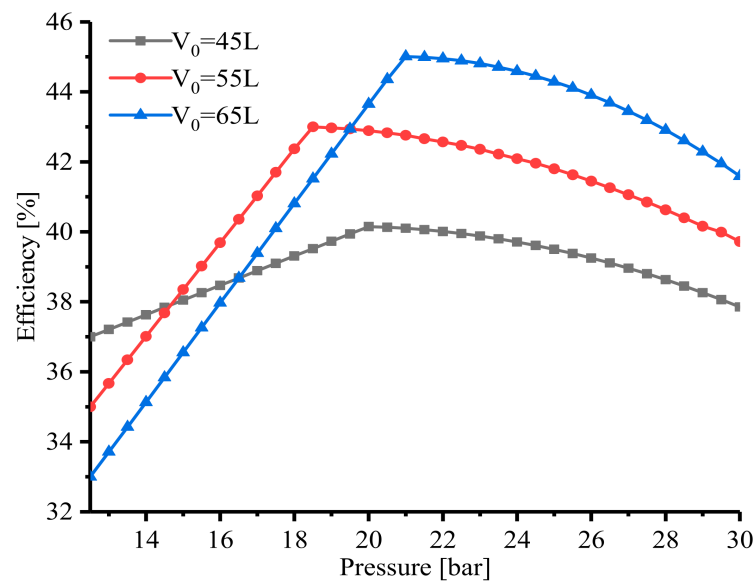


**Figure 15.** Accumulator variable filling pressure energy recovery efficiency curves.

#### 6.1.2. Analysis of the Effect of the Rated Volume of the Accumulator on Energy Recovery

Similarly, keeping the system's other parameters unchanged, the accumulator's volume is rated at 35 L to 75 L. The energy recovery efficiency of the system is analyzed under the accumulator filling pressure of 13 bar, 18 bar, and 23 bar. Figure 16 shows the accumulator variable volume energy recovery efficiency curves. The energy recovery efficiency of the system shows a rising and then decreasing trend as the rated volume of the accumulator rises. As the accumulator filling pressure increases, the system energy recovery efficiency gradually increases. Therefore, the system can improve energy recovery efficiency by increasing the rated volume of the accumulator.

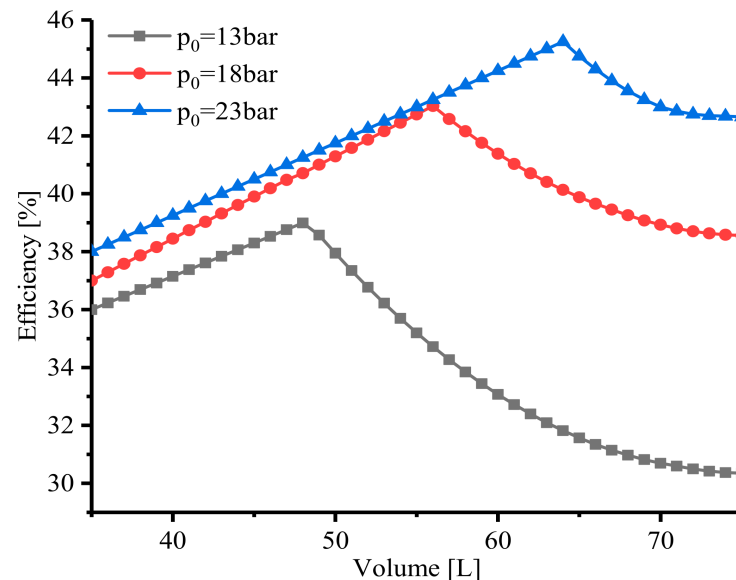


**Figure 16.** Accumulator variable volume energy recovery efficiency curves.

#### 6.1.3. Analysis of Energy Regeneration Hydraulic Motor Displacement on Energy Regeneration

Similarly, keeping the system's other parameters unchanged, the energy regeneration hydraulic motor displacement is rated at 50 mL/rev to 200 mL/rev. Furthermore, we analyzed the energy regeneration efficiency of the system under the working pressure



of 40 bar, 45 bar, and 50 bar after energy recovery from the accumulator gas. Figure 17 shows the energy regeneration hydraulic motor variable displacement energy regeneration efficiency curves. The energy regeneration efficiency of the system shows a rising and then maintaining trend as the hydraulic motor displacement rises. When the hydraulic motor displacement rises to 130 mL/rev, the working pressure after the accumulator energy recovery is not affected by the energy regeneration efficiency. Therefore, the system can improve the system energy regeneration efficiency by increasing the energy regeneration through hydraulic motor displacement.

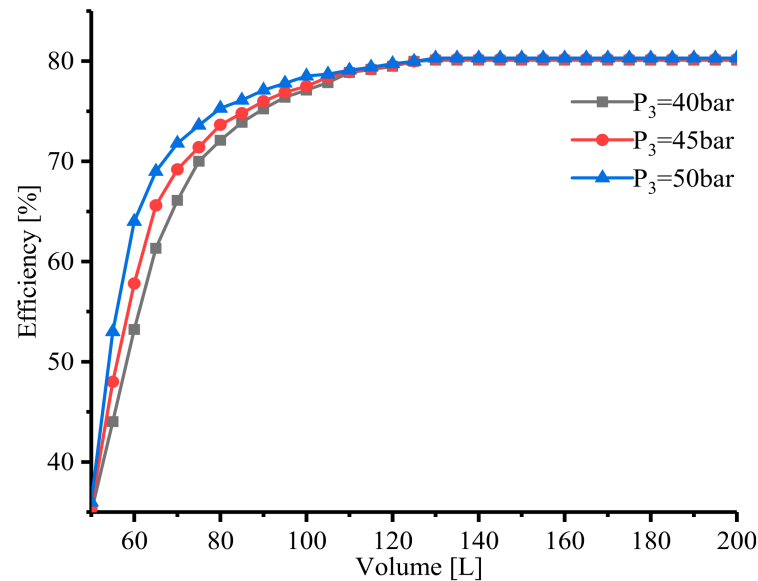


**Figure 17.** Energy regeneration hydraulic motor variable displacement energy regeneration efficiency curves.

Based on the above Section 6.1 analysis combined with Sections 3.3 and 3.4 analyses, the accumulator filling pressure is set to 23 bar. Additionally, considering the accumulator type, the accumulator's rated volume is set to 63 L. The energy regeneration hydraulic motor displacement is set to 130 mL/rev.

### 6.2. Analysis of System Energy Recovery and Regeneration after Parameter Optimization

Figure 18 shows the accumulator gas pressure, volume, and power curves after parameter optimization. The system performs energy regeneration between 5 s and 11 s. The accumulator gas pressure reduces from 49.9 bar to 13 bar. The accumulator gas fill percentage increases from 58.5% to 100%. The accumulator discharges power reduces from 24.2 kW to 8.1 kW. The system performs energy recovery between 17 s and 23 s. The accumulator gas pressure increases from 23 bar to 50 bar. The accumulator gas fill percentage reduces from 100% to 59.3%. The accumulator charges power increases from 9.2 kW to 25.2 kW. Combined with the analysis in Figure 13, it can be observed that the parameter optimization effectively improves the accumulator charging and discharging power.

Figure 19 shows the comparison curves of accumulator recovery and regeneration after parameter optimization. Before the parameter optimization, the energy recovered by the accumulator was 69.2 kJ, and the energy gained by the torque coupler was 51.8 kJ. After the parameter optimization, the energy recovered by the accumulator is 90.1 kJ, and the energy gained by the torque coupler is 72.4 kJ. The energy recovered by the accumulator is increased by 20.9 kJ, and 22.6 kJ increases the energy gained by the torque coupler.

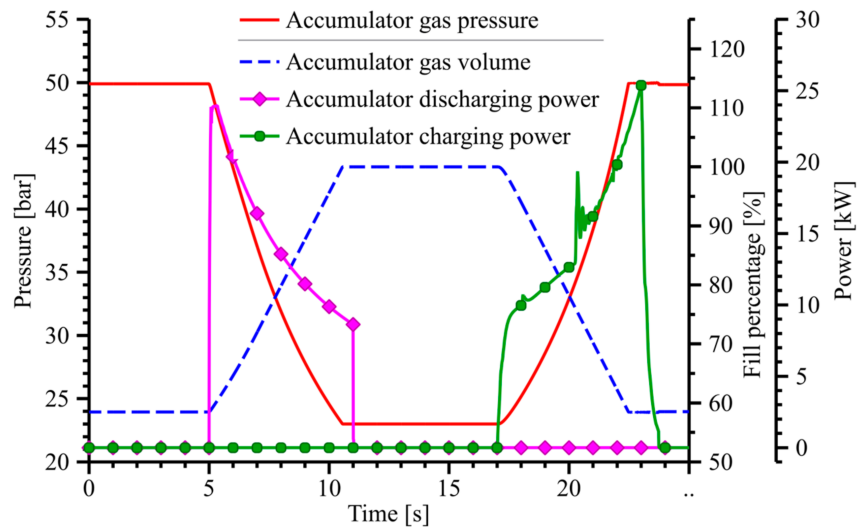


Figure 18. Accumulator gas pressure, volume and power curves after parameter optimization.

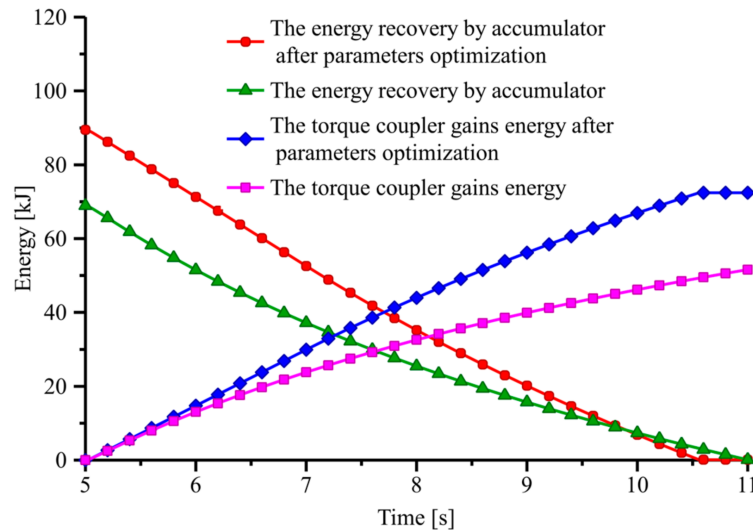


Figure 19. Comparison curves of accumulator recovery and regeneration after parameter optimization.

Figure 20 shows the system’s energy recovery and regeneration curves after parameter optimization. The total recoverable energy of the boom cylinder is 630.5 kJ, the total recover energy of the accumulator is 285.7 kJ, and the energy recovery efficiency of the system is 45.3%. The total energy released by the accumulator is 280.3 kJ, the total energy gained by the torque coupler is 223.7 kJ, and the energy regeneration efficiency is 79.8%. Combined with the analysis in Figure 14, the system energy recovery efficiency is increased by 9.8%, and the system energy regeneration efficiency is increased by 5.4%.

In summary, the accumulator charging and discharging power, recovery energy, and regeneration energy is significantly improved after parameter optimization. The system energy recovery and energy regeneration efficiency are improved.

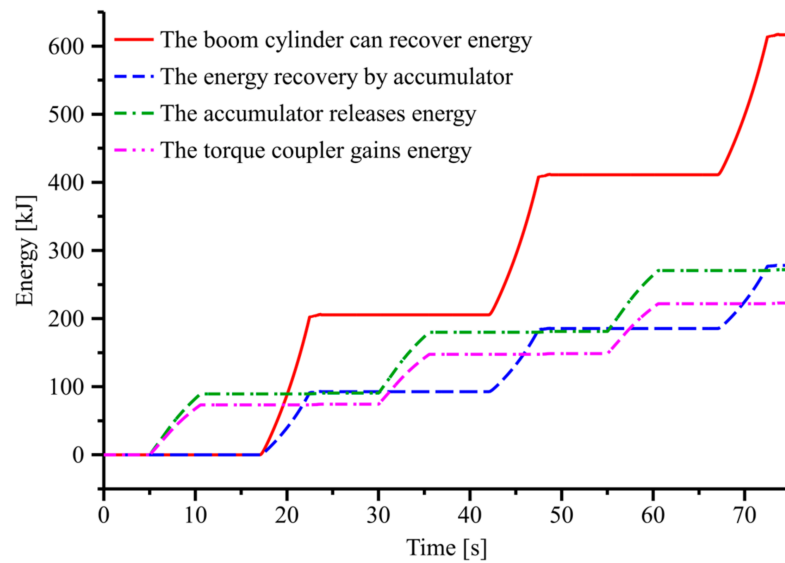


Figure 20. Energy recovery and regeneration curves of the system after parameter optimization.

## 7. System Energy-Saving Analysis

### 7.1. Engine Power Analysis

Figure 21 shows the engine power comparison curves. The maximum engine power of the conventional system, the hybrid system, and the hybrid system after parameter optimization is 67.7 kW, 43.5 kW, and 38.9 kW, respectively, when the boom arm rises between 5 s and 11 s. The maximum engine power is reduced by 35.7% before the parameter optimization and 42.5% after the parameter optimization of the hybrid system compared to the conventional system. The engine's maximum power is reduced by 6.8% after parameter optimization. When the boom arm drops, the accumulator is charged between 17 s and 23 s. The pressure of the accumulator gas gradually increases during the charging process, increasing the pressure of the piston side of the boom arm cylinder, which increases the outlet pressure of the load-sensing pump. Since the output flow rate of the pump is constant, the pump's output power increases, leading to an increase in engine output power. In summary, the hybrid system can effectively reduce the engine power when the boom arm rises.

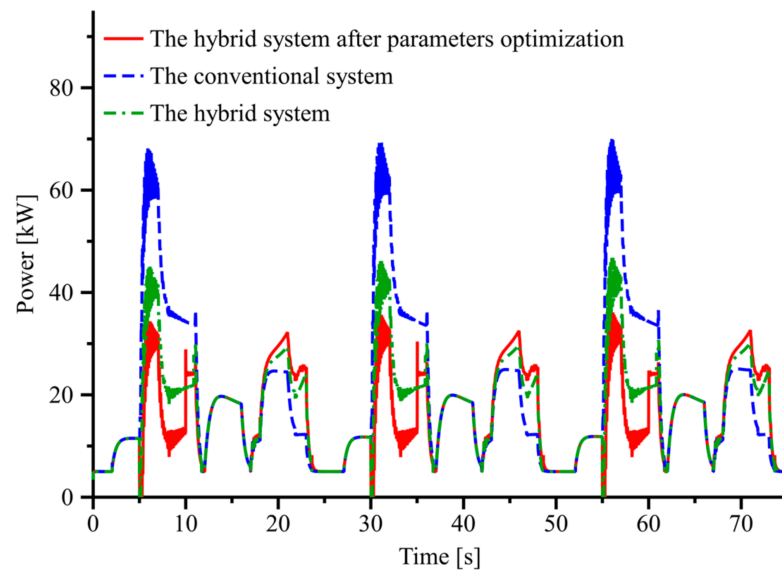


Figure 21. Engine power comparison curves.

## 7.2. Engine Fuel Consumption Analysis

The engine fuel consumption from Equation (1) is shown in Figure 22. The engine fuel consumption of the conventional system, the hybrid system, and the hybrid system after parameter optimization is 183 g, 155.3 g, and 146.2 g, respectively. The hybrid system reduces fuel consumption by 15.1% compared to the conventional system. The hybrid system after parameter optimization reduces fuel consumption by 20.1% after parameter optimization. Therefore, the engine fuel consumption is reduced by 5% after parameter optimization. In summary, the hybrid system can effectively reduce the engine fuel consumption.

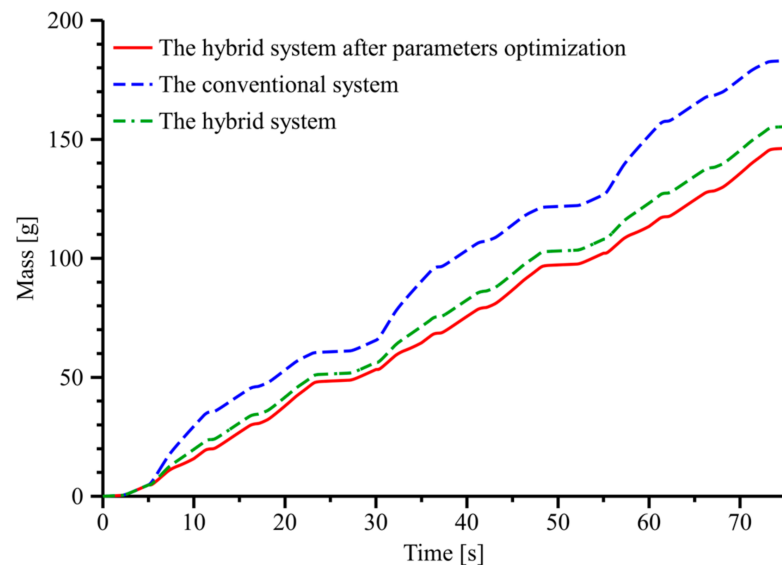


Figure 22. Engine fuel consumption comparison curves.

## 8. Conclusions

The principle of the hybrid loader boom arm energy recovery and regeneration system is analyzed. The system model is established and simulated under typical working conditions, and the system parameters are optimized and analyzed. The following conclusions can be obtained:

1. The system actuator is responsive and can meet the regular operation needs of the loader.
2. The energy recovery efficiency of the system shows a rising and then decreasing trend as the accumulator filling pressure and the rated volume of the accumulator rise. The energy regeneration efficiency of the system shows a rising and then maintaining trend as the hydraulic motor displacement rises.
3. The system energy recovery and energy regeneration efficiency reaches the maximum when the accumulator filling pressure is 23 bar, the rated volume is 63 L, and the energy regeneration hydraulic motor displacement is 130 mL/rev.
4. After optimizing the system parameters, the system energy recovery efficiency is 45.3%, and the system energy regeneration efficiency is 79.8%. The system energy recovery and regeneration efficiency have increased by 9.8% and 5.4%, respectively.
5. When the boom arm rises, the hybrid system can effectively reduce the engine power by 42.5% after parameter optimization. The system engine power is reduced by 6.8%.
6. The system can effectively reduce the engine fuel consumption by 20.1% after parameter optimization. The engine fuel consumption is reduced by 5%.
7. The system provides a reference for designing an energy recovery system and researching the energy-saving technology of loaders.

**Author Contributions:** Conceptualization and methodology, H.M.; software, validation, and writing—original draft preparation, H.M. and Y.L. (Yu Luo); writing—review and editing and supervision, project administration and funding acquisition, Y.L. (Yanlei Luo), Y.L. (Yu Luo) and L.C. All authors have read and agreed to the published version of the manuscript.

**Funding:** Research is funded by the Key Topics of Teaching Reform of Postgraduate Education in Guizhou Province (YJSCXJH (2020) 006), Science and Technology Project of Guizhou Province (Qiankehe Foundation-ZK [2022] General 087), National Natural Science Foundation of China Project (51965011), the State Scholarship Fund of China (201906675018).

**Data Availability Statement:** Data sharing is not applicable.

**Acknowledgments:** We would like to express our gratitude to the anonymous reviewers and friends who helped us in the process of completing this paper.

**Conflicts of Interest:** The authors declare no conflict of interest.

## References

1. Ranjan, P.; Wratt, G.; Bhola, M.; Mishra, S.K.; Das, J. A Novel Approach for the Energy Recovery and Position Control of a Hybrid Hydraulic Excavator. *ISA Trans.* **2019**, *99*, 387–402. [[CrossRef](#)] [[PubMed](#)]
2. Luxing, L. Research on Energy Recovery and Reuse of Parallel Hydraulic Hybrid Loader. Master's Thesis, Yanshan University, Qinhuangdao, China, 2021.
3. Quanming, Z.; Jinxia, Y.; Binqiang, Z. Research on braking energy recovery system of hydrostatic loader. *Constr. Mach. Equip.* **2021**, *52*, 93–99+12.
4. Chen, Q.; Lin, T.; Ren, H.; Fu, S. Novel potential energy regeneration systems for hybrid hydraulic excavators. *Math. Comput. Simul.* **2019**, *163*, 130–145. [[CrossRef](#)]
5. Yanlei, L.; Shanxu, Z.; Li, D.; Kun, L. Analysis of energy recovery system of hybrid agricultural loader. *Chin. Hydraul. Pneum.* **2021**, *45*, 109–114.
6. Xue, L. Research on Energy Management Control Strategy of Hybrid Wheel Loader. Master's Thesis, Jilin University, Changchun, China, 2021.
7. Jinxiao, G.; Lianpeng, X.; Lei, G.; Long, Q.; Xiaogang, Z. Operation and energy efficiency characteristics of large-scale mining hydraulic excavator boom. *Chin. Hydraul. Pneum.* **2022**, *46*, 108–115.
8. Jiansong, L.; Shaohui, L.; Bo, Z.; Jinhai, S.; Yuefeng, J. Design of flywheel based energy recovery system integrating flow regeneration for excavators. *Chin. Hydraul. Pneum.* **2020**, *5*, 68–74.
9. Che, G. Research on Electric Energy Recycling System of Electric Drive Hydraulic Excavator Boom. Master's Thesis, Taiyuan University of Technology, Taiyuan, China, 2020.
10. Haoqin, M. Research on Energy Regeneration of Excavator Boom Based on Constant Pressure Accumulator. Master's Thesis, Taiyuan University of Science and Technology, Taiyuan, China, 2020.
11. Yang, L. Research on energy-saving simulation of rotary device of hydraulic excavator based on energy recovery. Master's Thesis, University of South China, Hengyang, China, 2019.
12. Kaoshima, M.; Komiyama, M.; Nanjo, T.; Tsutsui, A. Development of New Hybrid Excavator. *Kobelco Technol. Rev.* **2007**, *27*, 39–42.
13. Weichao, S.; Huijun, G.; Okyay, K. Vibration isolation for active suspensions with performance constraints and actuator saturation. *IEEE Trans. Mech.* **2015**, *20*, 675–683.
14. Weichao, S.; Huijun, G.; Okyay, K. Finite frequency h $\infty$  control for vehicle active suspension systems. *IEEE Trans. Control Syst. Technol.* **2011**, *19*, 416–422.
15. Xiaogang, Z.; Xiangyu, W.; Hongjuan, Z.; Long, Q. Characteristics of wheel loader lifting device based on closed pump-controlled three-chamber hydraulic cylinder. *Trans. Chin. Soc. Agric. Mach.* **2019**, *50*, 410–418.
16. Xiangyun, S. Research on forward Modeling and Simulation for Hybrid Loader. Master's Thesis, Jilin University, Changchun, China, 2019.
17. Hui, S.; Jing, J. Research on the System Configuration and Energy Control Strategy for Parallel Hydraulic Hybrid Loader. *Autom. Constr.* **2010**, *19*, 213–220. [[CrossRef](#)]
18. Dandan, Z.; Xuwei, Z.; Wei, Z. Double accumulator for parallel hydraulic hybrid vehicle braking characteristics. *Chin. Hydraul. Pneum.* **2015**, *2*, 74–78.
19. Tianliang, L.; Qiang, C.; Haoling, R.; Weiping, H.; Qihuai, C.; Shengjie, F. Boom energy recovery system with auxiliary throttle based on hybrid excavator. *Proc. Inst. Mech. Eng. Part C J. Mech. Eng. Sci.* **2016**, *231*, 4250–4262. [[CrossRef](#)]
20. Mandal, P.; Sarkar, B.K.; Saha, R.; Chatterjee, A.; Mookherjee, S.; Sanyal, D. Real-time fuzzy-feedforward controller design by bacterial foraging optimization for an electrohydraulic system. *Eng. Appl. Artif. Intell.* **2015**, *45*, 168–179. [[CrossRef](#)]
21. Venkaiah, P.; Sarkar, B.K. Electrohydraulic proportional valve-controlled vane type semi-rotary actuated wind turbine control by feedforward fractional-order feedback controller. *Proc. Inst. Mech. Eng. Part I J. Syst. Control Eng.* **2022**, *236*, 318–337. [[CrossRef](#)]
22. Tianliang, L. Research on the potential energy regeneration system based on the hybrid hydraulic excavators. Ph.D. Thesis, Zhejiang University, Hangzhou, China, 2011.



23. Ge, L.; Quan, L.; Li, Y.; Zhang, X.; Yang, J. A novel hydraulic excavator boom driving system with high efficiency and potential energy regeneration capability. *Energy Convers. Manag.* **2018**, *166*, 308–317. [[CrossRef](#)]
24. Jinxia, L.; Zhiyuan, J.; Fangxin, X.; Wenting, L. Energy recovery and utilization system of excavator boom based on flow regeneration and balance theory. *J. Braz. Soc. Mech. Sci. Eng.* **2020**, *42*, 1–11.
25. Lin, T.; Chen, Q.; Ren, H.; Zhao, Y.; Miao, C.; Fu, S.; Chen, Q.H. Energy regeneration hydraulic system via a relief valve with energy regeneration unit. *Appl. Sci.* **2017**, *7*, 613. [[CrossRef](#)]
26. Liu, X. Study on the Energy Characteristics of Working Device Hydraulic System for 50-type loaders. Master's Thesis, Jilin University, Changchun, China, 2017.
27. Wang, C. Research on Hybrid Pressure Compensated Hydraulic Control System. Master's Thesis, Guizhou University, Guiyang, China, 2021.